Critical behavior of a two-dimensional complex fluid: Macroscopic and mesoscopic views

Madhumita Choudhuri and Alokmay Datta*

Surface Physics and Material Science Division, Saha Institute of Nuclear Physics, 1/AF Bidhannagar, Kolkata 700064, India

(Received 31 December 2015; revised manuscript received 16 February 2016; published 13 April 2016)

Liquid disordered (L_d) to liquid ordered (L_o) phase transition in myristic acid [MyA, $CH_3(CH_2)_{12}COOH$] Langmuir monolayers was studied macroscopically as well as mesoscopically to locate the critical point. Macroscopically, isotherms of the monolayer were obtained across the 20 °C–38 °C temperature (T) range and the critical point was estimated, primarily from the vanishing of the order parameter, at ≈38 °C. Mesoscopically, domain morphology in the L_d-L_o coexistence regime was imaged using the technique of Brewster angle microscopy (BAM) as a function of T and the corresponding power spectral density function (PSDF) obtained. Monolayer morphology passed from stable circular domains and a sharp peak in PSDF to stable dendritic domains and a divergence of the correlation length as the critical point was approached from below. The critical point was found to be consistent at ≈38 °C from both isotherm and BAM results. In the critical regime the scaling behavior of the transition followed the two-dimensional Ising model. Additionally, we obtained a precritical regime, over a temperature range of ≈8 °C below T_c, characterized by fluctuations in the order parameter at the macroscopic scale and at the mesoscopic scale characterized by unstable domains of fingering or dendritic morphology as well as proliferation of a large number of small sized domains, multiple peaks in the power spectra, and a corresponding fluctuation in the peak q values with T. Further, while comparing temperature studies on an ensemble of MyA monolayers with those on a single monolayer, the system was found to be not strictly ergodic in that the ensemble development did not strictly match with the time development in the system. In particular, the critical temperature was found to be lowered in the latter. These results clearly show that the critical behavior in fatty acid monolayer phase transitions have features of both complex and nonequilibrium systems.

DOI: 10.1103/PhysRevE.93.042804

I. INTRODUCTION

Phase transitions can be described by the change in an order parameter associated with a system [1–4]. At macroscopic length scales, quantities that are essentially derivatives of the order parameter with respect to the thermodynamic variables, such as compressibility or susceptibility, diverge as the critical point is approached, as typical exponents of the differences between the variables and their critical values. We would like to denote this description of critical behavior as a "thermodynamic" or "macroscopic" description or view. Simultaneously, as the critical point is approached, there are characteristic changes in the statistical behavior of the system. The interfacial energy becomes as low as the thermal energy k_BT so that large thermally driven fluctuations in the order parameter, spanning from microscopic to macroscopic length scales, develop in the system and the correlation length of these fluctuations also diverge. This behavior may be called the "statistical" or "mesoscopic" view of critical behavior.

While the critical behavior of three-dimensional systems is well known from both the macroscopic and mesoscopic views and they are found to be consistent, not many reports regarding the same for two-dimensional (2D) systems is found [5–10]. The nearest 2D analog of a fluid that can be realized and maintained at ambient conditions is the Langmuir monolayer, a single layer of amphiphilic molecules stabilized at the water surface through the competing forces of attraction of one part ("head," hydrophilic COOH, OH, or ester groups) and the repulsion of the other ("tail," hydrophobic hydrocarbon chain) to water [11,12]. If the tail length is less than 16 carbon atoms, such monolayers show a first order transition from a "liquid disordered" or L_d phase with tails having short range tilt order but with both *trans* and *gauche* conformations of the CH_2 groups in the tails to a "liquid ordered" or L_o phase where the tails are all in *trans* conformation and have long-range tilt orientation order. An extensive study of the phase transitions in fatty acid monolayers and the distinct textures associated with the various phases of the monolayer domains was carried out using the techniques of Brewster angle microscopy (BAM) as well as polarized fluorescence microscopy (PFM) by Knobler *et al.* [13]. In lipids such as phospholipids, each molecule has two tails instead of the single one in the examples above. For them also the L_d to L_o transition is present.

Unfortunately, there is an absence of studies on the critical behavior of pure fatty acids and, in fact, pure single tailed amphiphilic monolayers, as far as we can find. The only other study of the phenomena in pristine monolayers was done by Nielsen *et al.,* in which the group reported 2D critical points in monolayers of the phospholipids (two tailed amphiphiles), dimyristoyl phospatidylcholine (DMPC), and dipalmitoyl phospatidylcholine (DPPC), where they reported a divergence of the correlation length at T_c (20 °C for DMPC and 39 °C for DPPC), apparently in accordance with 3D systems [14,15]. This result underscores the relevance of studying the critical behavior of these easily achievable 2D systems, in particular if we consider that in this work the lateral structure of the monolayers at the critical point was probed by atomic force microscopy only after transferring the films onto solid substrates and that reports of *in situ* visualization and study of critical behavior in Langmuir monolayers are hard to come by.

*alokmay.datta@saha.ac.in

Isotherms of Langmuir monolayers of an amphiphilic fatty acid [myristic acid, MyA, $CH_3(CH_2)_{12}COOH$] were first studied over the extensive temperature range of 2.5 °C to 34.4 °C in the 1920s by Adam and Jessop [16]. They found the L_d to L_o (LE-LC or liquid expanded to liquid condensed in the old terminology) transition, where (1) the coexistence region was not completely flat, i.e., the 2D compressibility in this region [$\kappa \equiv -1/A(\partial A/\partial \pi)$] was nondivergent; (2) the shrinking of the coexistence region with temperature was accompanied by a continuous but small increase in the slope of this region or a decrease in κ; and (3) absence of this region until $\pi \sim 28$ mN/m (the highest value of π measured by them). Also, they did not report any isotherm between 26.2 °C and 34.4 °C. These early results were used by Suresh *et al.* as the basis for a fluorescent microscopic study of the L_d to L_o transition of MyA [17]. In particular, they adopted 31 °C as the critical temperature (T_c). In their study they doped the monolayer with an amphiphilic fluorescent dye (4-hexadecylamino-7-nitrobenz-2oxa-1,3 diazole) and monitored the change of L_o domain patterns during the L_d to L_o phase transition as a function of temperature. Primarily, the study indicated the formation of circular L_o phase domains within the L_d phase below 31 °C, which change to self-similar fingering domains of L_o over a 5 °C temperature range as this T_c designated by them is approached from below. A study on microscopic pattern formation on MyA monolayer was also carried out by Akamatsu *et al.* [18]. This study, however, had no mention of critical behavior in the monolayer.

It is apparent that for understanding the basics of *critical behavior in 2D* of any intrinsic phase transition of monolayers in general, and of pristine monolayers in particular, the monolayers need to be investigated on the water surface, thereby allowing for the natural dynamics. Further, single tailed amphiphilic fatty acids are perhaps one of the "simplest complex systems" for study and can serve as the basis for understanding more complex systems.

We have chosen the fatty acid MyA for our studies because it shows a prominent L_d to L_o first order, chain ordering phase transition. Long tailed fatty acids do not exhibit this transition, which is otherwise also observed in lipid monolayers. As pointed out earlier, for pristine Langmuir monolayers in general, there are only a few studies and for this transition in particular, there are no *in situ* studies that combine isotherm measurements with structural imaging and thus present a complete picture from both macroscopic and mesoscopic view points. We have made a systematic study of both surface pressure *versus* specific molecular area ($\pi - A$) isotherms and data obtained from structural imaging, at various temperatures in order to locate the critical point and study the approach toward criticality of the system. For the mesoscopic view we have employed Brewster angle microscopy, which does not require any contaminating fluorescent dye and hence is a better technique compared to fluorescence microscopy used in the earlier work on the MyA monolayer mentioned above. In our studies we have combined the data obtained from the two techniques and found well defined L_o and L_d phase domains at temperatures far below T_c and a single phase above T_c with the approach towards criticality being associated with a fluctuating precritical regime which occurs within a temperature range of 8° below the critical point. We also found that the value of T_c varied from ≈36 °C to ≈38 °C depending on the preparation of the system, pointing to the essentially nonequilibrium nature of Langmuir monolayers.

II. EXPERIMENTAL DETAILS

Langmuir film preparation and isotherm measurements. The Langmuir trough (Nima Technologies) was repeatedly rinsed with MilliQ water to free it of contaminants. It was then wiped with tissues (low lint Kimtech) soaked in chloroform (Merck-Emplura, purity $\geqslant$ 99%) and subsequently in 2-propanol (Merck-Emplura, purity $\geqslant$ 99%) to ensure removal of any remaining impurities. The water used in our experiments was MilliQ, resistivity 18 MΩ cm, collected in a Borosil glass jar just prior to the experiments. After filling the trough to the brim with water, the barriers were compressed to the minimum trough area (≈60 cm^2). The water surface was then cleaned and tested for surface impurities following the surface pressure test where the water surface was repeatedly aspirated, with barriers fully closed (the minimum trough area), until the difference between the surface pressure values when the barrier was fully open (maximum trough area) and fully closed (minimum trough area) was $\leqslant 0.1$ mN m^{-1}. The Langmuir trough and the microscope were enclosed in a glass casing to minimize any surface contamination during the experiment and the experiments were started after sufficient time to make the surface come to equilibrium with the water vapor. A chloroform solution (100 μL) of myristic acid (Sigma grade, purity $\geqslant$ 99%) of concentration 1 mg/ml was spread using a Hamilton syringe on the water surface, without further purification of the acid. The amphiphilic fatty acid molecules self-assembled into a monolayer at the air-water interface. The temperature (T) was regulated with a temperature controller (Julabo GmbH, Germany) and we waited for 15 min for the subphase to reach the desired temperature set by the controller, before spreading the fatty acid monolayer. The chloroform evaporated within 10 min, after which the film was compressed by moving inward the trough barriers at 0.5 cm/min. The surface pressure π was monitored as a function of the monolayer covered trough area as well as the specific molecular area (A). These $\pi - A$ isotherms were obtained at several temperatures ranging from 20 °C to 38 °C. The temperature studies are divided into two sections, namely "Temperature studies on different MyA monolayers" and "Temperature studies on a single MyA monolayer." In the former case, after setting the desired temperature with the controller, the monolayer was compressed isothermally and images recorded during ongoing compression. This was repeated at different temperatures for different MyA monolayers. In the latter case a single monolayer was compressed until the π value of L_d to L_o coexistence was reached and thereafter the temperature was increased in small steps and the corresponding monolayer response was recorded.

Brewster angle microscopy. An imaging ellipsometer (Accurion GmbH, Germany) was employed in the Brewster angle microscopy mode for visualization of the films on the surface of water, on a scale of few hundred μm with an in plane resolution of 0.455 μm [19,20]. The microscope works in the reflection mode and employs monochromatic p-polarized laser light (658 nm) incident at the Brewster angle of water to

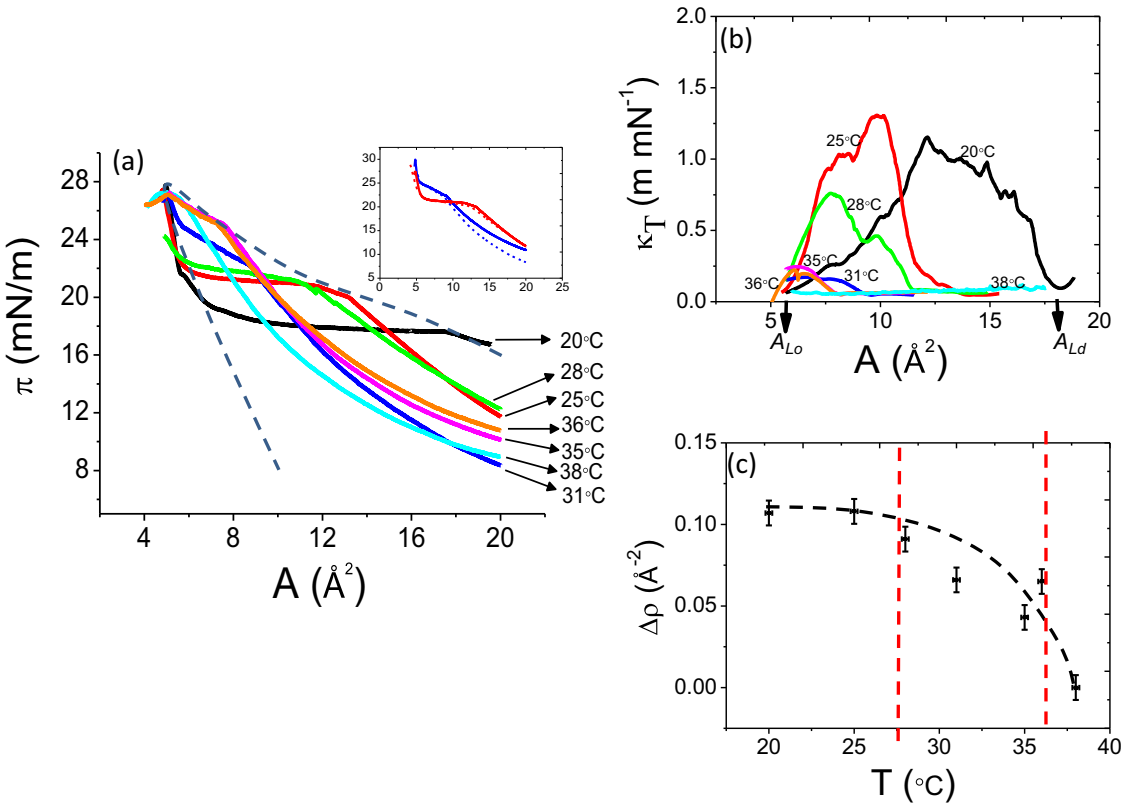

FIG. 1. (a) Surface pressure versus specific molecular area ($\pi - A$) isotherms of MyA at 20 °C (black), 25 °C (red), 28 °C (green), 31 °C (blue), 35 °C (magenta), 36 °C (orange), and 38 °C (cyan) exhibiting a critical point at $T_c = 38$ °C. Also, the envelope of the coexistence regions across the T range is shown by the dashed curve. The inset shows isotherms of two different monolayers (shown by solid and dotted lines) at 25 °C (red, broader plateau) and 31 °C (blue). (b) Compressibility (κ_T) plotted as a function of temperature T; arrows show A_{L_d} and A_{L_o} for $T = 20$ °C. (c) Average surface number density difference ($\Delta\rho$) between the L_o and L_d phases. Panel (c) shows the data (solid circles), the error bars, the mean curve (dashed line), and the precritical fluctuating regime marked between the vertical lines for virtual clarity. The error bars for the temperature measurements merge with the symbols for averages.

extinguish the background refection from the water subphase. The local refractive index at the film is different from that of the bare water surface, causing light to be reflected, thus making the film visible.

III. RESULTS AND DISCUSSION

A. Isotherm measurements: Macroscopic view of criticality

The $\pi - A$ isotherms of the MyA monolayer at various temperatures between 20 °C and 38 °C are shown in Fig. 1(a). A plateau in each of the isotherms close to $\pi \approx 20$ mN m^{-1} corresponds to the L_d to L_o phase transition in the monolayer. Our isotherms are consistent with those of previous investigations until 34.4 °C [16], the highest temperature data recorded so far, and they are also fairly reproducible especially at low temperatures, as can be seen from inset in Fig. 1(a). The isotherm at 20 °C is characterized by the broadest and flattest plateau that occurs at 17 mN m^{-1} [Fig. 1(a)]. With an increase in temperature two notable changes occur: (1) The coexistence plateau progressively shrinks along the specific molecular area (A) axis and finally vanishes at 38 °C, thereby indicating the existence of a critical point around this temperature; (2) there is an increase in the absolute value of slope ($-\partial\pi/\partial A$) of the isotherm and thereby a decrease in compressibility $\kappa[-1/A(\partial A/\partial\pi)]$ in the coexistence region, the second feature coming from the long-range dipolar repulsion of the head groups [21,22]. Another feature that is worth mentioning is the asymmetric nature of the curve enveloping the coexistence regions across T [dashed curve in Fig. 1(a)], which has already been pointed out for phase transitions in Langmuir monolayers in several of the early works on this subject and is a consequence of the fact that, unlike in 3D gas to liquid phase transitions, where the term b in van der Waals equation of state accounting for the excluded volume is a constant, in 2D this term representing the excluded area is a decreasing function of the surfactant density (b is larger in the L_d phase, where the tails lie almost flat on the water surface, compared to the L_o phase, where they are vertical) [23].

Based on the isotherm measurements it becomes necessary to assign a suitable order parameter to this phase transition, a parameter that distinguishes the two phases below the critical point and vanishes at the critical point. The average surface number density difference ($\Delta\rho = 1/A_{L_o} - 1/A_{L_d}$) between the L_d and L_o phases is plotted as a function of temperature (T) in Fig. 1(c). A_{L_d} and A_{L_o} are the A values just before and after the monolayer enters and exits, respectively, the coexistence π regime in the isotherm. In order to precisely locate this pair of points, we obtained the isothermal compressibility κ_T at different temperatures [Fig. 1(b)]. Since the coexistence

region appears as a plateau in these curves, A_{L_d} and A_{L_o} were obtained as the pair of points that lie at the feet of this plateau on either side, an example shown by arrows for $T = 20\,^{\circ}$C in Fig. 1(b). The graphs in Fig. 1(b) have, in turn, been obtained by calculating the local slope at each point along the isotherms at various T. The graphs are presented here after smoothing (Savitzky Golay method with 200 window points, using the ORIGINPRO 8.5 software). Error limits in $\Delta\rho$ and T were estimated using standard methods, assuming the error in measuring A to be the major source of error for the former.

$\Delta\rho$ decreases between 25 °C and 28 °C, fluctuating between 28 °C and 36 °C before becoming 0 at the estimated critical point. Since it disappears at and has a nonzero value below the estimated critical point, $\Delta\rho$ can be treated as an order parameter for this transition. It shows a precritical region marked by fluctuations in the 28 °C to 36 °C temperature range before passing into the critical regime at around 38 °C.

We have observed that the average isothermal compressibility κ_T in the coexistence regime [shown in Fig. 1(b)] also shows a similar trend of a marked decrease between 25 °C and 28 °C and fluctuations between 28 °C and 36 °C before ending up at 0 at 38 °C. As discussed earlier, κ_T does not diverge in the coexistence regime because (unlike gases with only short range attraction) a long range dipolar repulsion exists between the head groups of MyA in such monolayers that needs to be overcome in order to cause transition to the more condensed phase. Pallas and Pethica [24] have shown that the shape of the isotherm (existence of a flat plateau or otherwise) during phase transitions in Langmuir monolayers could be significantly altered by the presence of impurities, the condition of surface vapor equilibrium as manifested by the relative humidity, and the precise way in which the film is compressed. However, we would like to point out that these considerations may not be relevant for our isotherms due to the following. (1) Our low temperature isotherms have a flat coexistence region and a systematic change to "tilted across the phase coexistence π regime" was repeatedly observed only at $T > 28\,^{\circ}$C (close to the precritical region), which cannot be explained by impurity or humidity factors, as all our experiments have been conducted under similar experimental conditions. It rather looks more like a thermodynamic feature dependent on temperature. In contrast, the tilt in the isotherm during the phase transition in pentadecanoic acid was found to depend on the relative humidity and apparently was not temperature dependent [24]. (2) The pentadecanoic acid monolayer [24] was maintained over water at a pH value 2, which prevented head-group dissociation, thus making $COO^{-}H^{+}$ dipoles to be the majority species and thereby lowering the long-range part of the interaction, whereas in our case the subphase was pristine water at ambient conditions, generally having pH $\sim$ 5.6, providing for sufficient head-group dissociation. We may add that our analysis and explanations are based on the shrinking of the coexistence region with temperature rather than the occurrence of tilt in this region. Nevertheless, due to the above controversy and the fact that we did not further purify the fatty acid, we refrain from assigning κ_T as an order parameter for this phase transition and stick to $\Delta\rho$ as our (unambiguous) macroscopic order parameter. In order to have a better understanding of both the precritical and critical regions as well as to confirm their existence, we carried out BAM studies on the monolayers.

B. Brewster angle microscopy: Mesoscopic view of criticality

1. *Temperature studies on several MyA monolayers*

Domain morphology. BAM images of six MyA monolayers maintained at six different temperatures between 20 °C and 38 °C, in the L_d to L_o coexistence regime of the monolayers are shown in Figs. 2(a)–2(f). Three distinct temperature regimes associated with distinct domain morphologies and sizes could be identified.

$T < T_c$. There are two temperature regimes in this region: T far below T_c ($T < 28\,^{\circ}$C) and T approaching T_c ($28\,^{\circ}\text{C} \leqslant T \leqslant 36\,^{\circ}$C).

(a) $T < 28\,^{\circ}C$ *[Figs. 2(a) and 2(b)].* Circular L_o domains formed, in the coexistence regime, for $T < 25\,^{\circ}$C [Fig. 2(a)]. On the higher side of this temperature regime, for $T > 25\,^{\circ}$C, circular domains became unstable and the domains between 25 °C and 28 °C exhibited noncircular fingerlike structures alongside circular ones [Fig. 2(b)].

(b) $28\,^{\circ}\text{C} \leqslant T \leqslant 36\,^{\circ}C$ *[Figs. 2(c)–2(e)].* The L_o phase, in general, showed fractal morphology. On the lower side of this temperature regime, the fractal domains rapidly reverted to circular structures within a few minutes, while, on the higher side, the fractal domains were stable for a longer period. In addition, between 31 °C and 36 °C, proliferation of a large number of small, nearly circular domains of varying sizes occurred.

$T \approx T_c$

(c) $36\,^{\circ}C < T < 38\,^{\circ}C$ *[Fig. 2(f)].* Domain morphology was dominated by stable fractal dendritic structures. The phase boundaries disappeared above 38 °C and domain structures were no longer discernible.

Radial power spectral density function. Statistical analysis of the 2D morphological evolution regimes requires the two-dimensional power spectral density function $W(q_x,q_y)$, which can be expressed as the Fourier transform of the autocorrelation function

$$W(q_x,q_y) = 1/4\pi \int\int_{-\infty}^{\infty} G(\delta_x,\delta_y) e^{-i(q_x\delta_x + q_y\delta_y)} d\delta_x d\delta_y, \quad (1)$$

where $\delta_x = x_1 - x_2$ and $\delta_y = y_1 - y_2$, x and y being the spatial coordinates. $G(\delta_x,\delta_y)$ is the intensity autocorrelation function, where intensity $I = 0$ and 1 at the pixel positions corresponding to the L_d and L_o phases, respectively, in the binarized images. The binarization process as shown in Fig. 3 was accomplished with the help of Image J software (software for image analysis developed by National Institutes of Health, USA).

However, the more relevant quantity is the radial power spectral density function (PSDF) or simply power spectra $W_r(q)$, which is the angularly integrated two-dimensional PSDF, i.e.,

$$W_r(q) = \int_0^{2\pi} W(q\cos\phi, q\sin\phi) q\, d\phi. \quad (2)$$

$W_r(q)$ for several temperatures between 20 °C and 38 °C are shown in Fig. 4(a) and peak positions at the corresponding T values are plotted in Fig. 4(b). $W_r(q)$ at a particular T is the

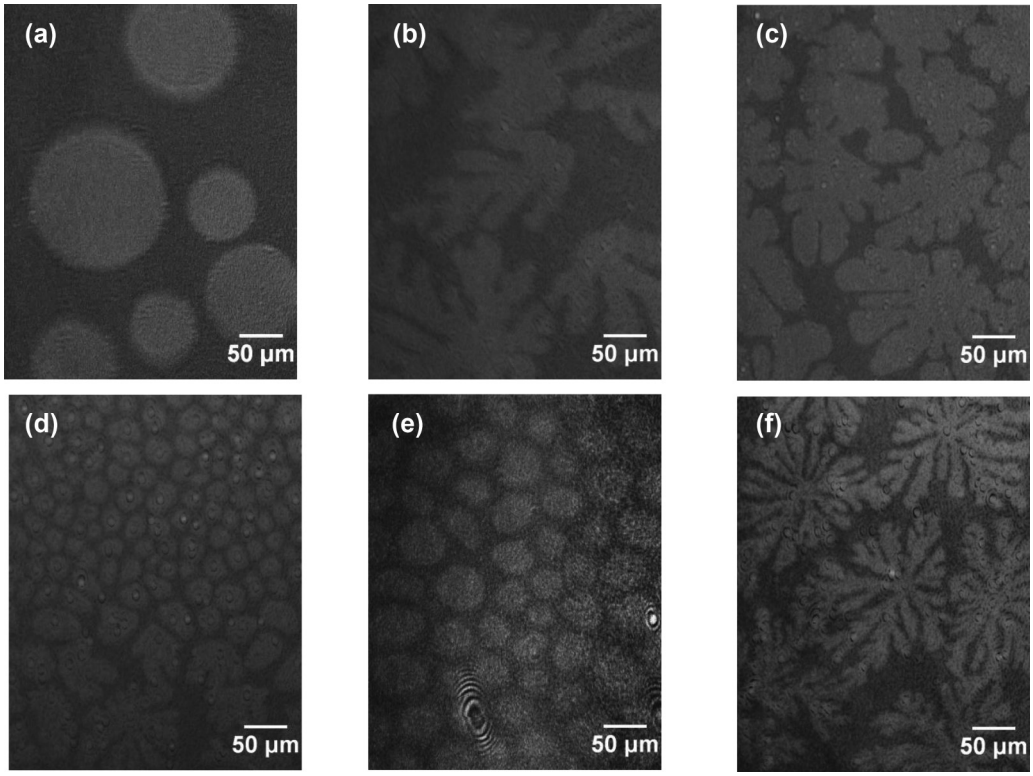

FIG. 2. Brewster angle microscopy (BAM) images of the MyA monolayer showing L_o phase domains of the monolayer coexisting with the L_d phase at (a) 17 mN m^{-1}, 20 °C, (b) 21 mN m^{-1}, 25°C, (c) 24 mN m^{-1}, 28 °C (d) 24 mN m^{-1}, 31 °C (e) 24 mN m^{-1}, 35 °C and (f) 27 mN m^{-1}, 38 °C.

average quantity computed over two binarized images in the coexistence region, using the GWYDDION 2.40 software (a data visualization and analysis tool). The power spectra are plotted for temperatures $T \approx T_c$, on a log-log scale, in Figs. 4(c) and 4(d), where the curves are upshifted by arbitrary amounts for visualization. The characteristics of the power spectra in the three temperature regimes already identified from the BAM images are as follows.

$T < T_c$. From the plots in Fig. 4, this region can be subdivided into two regimes, namely T far below T_c ($T <$ 28 °C) and T approaching T_c (28 °C $\leqslant T \leqslant$ 36 °C).

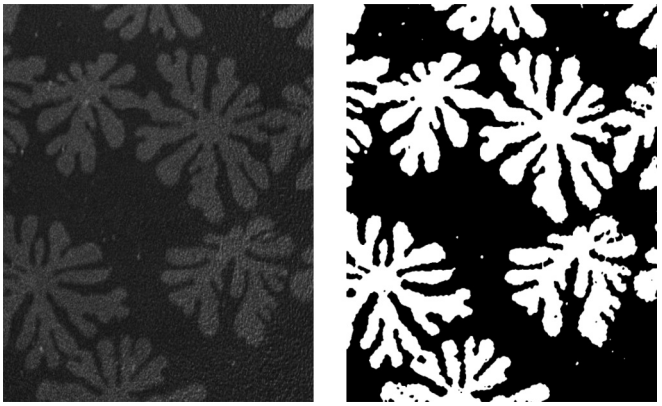

FIG. 3. Grayscale image (left) and the corresponding binarized image (right).

(a) $T < 28\,^{\circ}C$. $W_r(q)$ shows a single well defined peak for $T = 20$ °C and 25 °C at the q value 4.95×10^4 m^{-1}, which corresponds to a domain size of 128 μm.

(b) $28 \leqslant T \leqslant 36\,^{\circ}C$. Significant fall and broadening of the power spectra accompanied by the evolution of multiple peaks occurs with the onset of fractality at 28 °C. Simultaneously, the formation of a large number of small sized domains causes the power spectral peak at $T = 31$ °C to shift to higher q values. However, at still higher temperatures ($T \geqslant 35$ °C), closer to the critical point, the peak shifts to low q values. This regime, thus, shows fluctuations associated with a rise and fall in the peak q (q_p) position [Fig. 4(b)].

$T \approx T_c$

(c) $36\,^{\circ}C < T < 38\,^{\circ}C$. Close to the critical point the power spectra peak shifts towards 0 to lower q values. Since the power spectra represents the Fourier transform of the intensity autocorrelation in the image, a shift of the peak towards lower q values suggests long wavelength correlations in the intensity profile. In Fig. 4(b) this is represented by the lone point outside the fluctuation regime at 38 °C, corresponding to $q \approx 3.2 \times 10^4$ m^{-1} or equivalently correlated fluctuation of the size ≈196 μm. Such long wavelength components signify divergence of the correlation length near T_c. MyA monolayers were further investigated close to the critical point and the corresponding structure factors at 36.2 °C, 36.8 °C, 37 °C, and 37.5°C were plotted on a log-log scale in Figs. 4(c) and 4(d). Closest to the critical point at 37.5 °C, W_r scales as a power law as $W_r(q) \approx q^{2x}$, with $x \approx 1$. Our exponent matches with that already obtained for lipid monolayers [14] and confirms

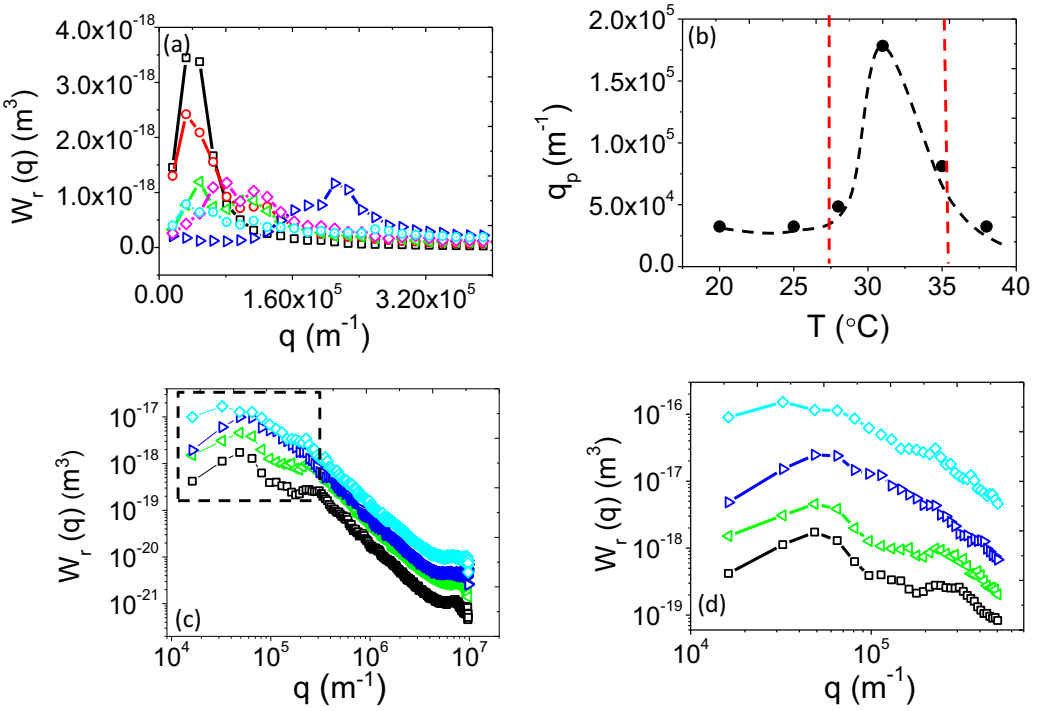

FIG. 4. (a) Power spectral density function (W_r) plotted as a function of q at temperatures 20 °C (black squares), 25 °C (red circles), 28 °C (green left triangles), 31 °C (blue right triangles), 35 °C (magenta diamonds), and 38 °C (cyan dotted circles). (b) Plot of the peak q position as a function of T (for multiple peaked spectra, peak position at the lowest q value is plotted) where the fluctuation regime is shown within vertical lines. (c) W_r plotted as a function of q on a log-log scale for $T \approx T_c$ at 36.2 °C (black squares), 36.8 °C (green left triangles), 37 °C (blue right triangles), 37.5 °C (cyan diamonds). Sections of the spectra (c), at low q values (in the dashed box), are shown in (d). The spectra in (c) and (d) are upshifted by arbitrary amounts for visualization.

that the MyA monolayer too conforms to the universality class of the 2D Ising model.

The mesoscopic studies of the MyA monolayer thus confirm the presence of a subcritical fluctuation regime extending over a temperature range of ≈8° below the critical point. $T \ll T_c$ is characterized by stable circular domains and a sharp peak in the power spectra with a single q_p, while $T \approx T_c$ is characterized by stable dendritic domains, power spectral peak nearing 0 along the q axis, and no well defined q_p, and the intermediate regime separating the two is characterized by unstable domains of fingering or dendritic morphology and proliferation of a large number of small sized domains, multiple peaks in the power spectra, and a corresponding fluctuation in q_p values along the temperature axis. The location of the three regimes obtained from Brewster angle microscopy studies match well with those obtained from the isotherm studies of the monolayer.

Comparison with lipid monolayer results apparently leads to the conclusion that for those monolayers this fluctuating or precritical regime has been identified with criticality. The question is whether this situation arises because (a) the monolayer on water was not studied beyond this precritical region or (b) the monolayer was studied mesoscopically only after it was transferred onto substrates. While it is difficult to rule out the first doubt without repeating the study, the second doubt can be set aside from considering the fact that the dendritic structures with MyA can be preserved, at least qualitatively upon transfer, as we have observed ourselves.

If, however, we *a priori* accept this identification of criticality of the lipid monolayer with the precriticality of the fatty acid monolayer, we also accept the inability of the former to form dendritic structures. This, then, is a fundamental difference between one tailed and two tailed complex fluids. We suggest that this comes from the surface correlation among the fatty acid tails, missing in the lipid tails, as the fatty acid tails are known [11] to close pack into 2D ordered phases. At criticality this tail tail interaction may translate into a Bethe lattice or Cayley tree like structure that shows up as the dendrites we have observed.

2. *Temperature studies on a single monolayer*

For the temperature studies reported in the previous sections, monolayers spread on water were maintained at desired temperature values and subsequently compressed quasistatically. Monolayers spread at several temperatures between 20 °C and 38 °C were studied during their isothermal compression and the data collated to obtain the response of the monolayer to an increase in temperature. Hence, the temperature studies were conducted on identical *copies* of the MyA monolayer that were maintained at several temperatures between 20 °C and 38 °C. However, another approach would be to test the response of a single MyA monolayer to an increase in temperature. This would enable us to test the ergodicity of the system that is whether the system has identical behavior when averaged over time as averaged over space of all the systems states. The monolayer was spread

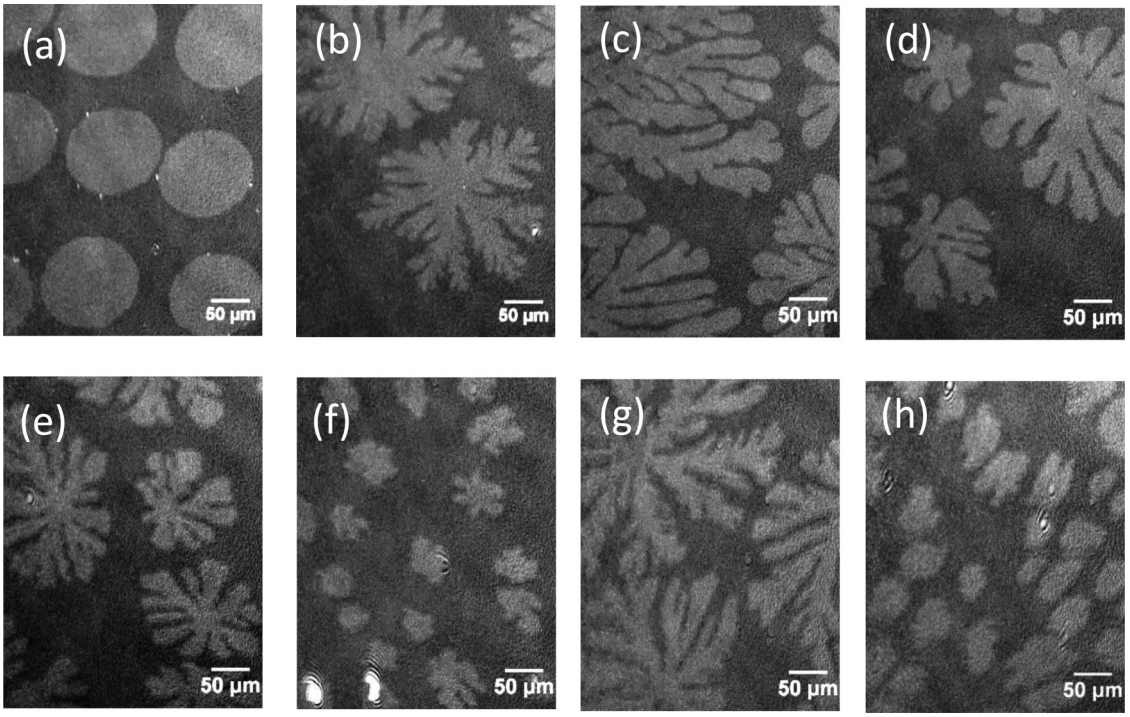

FIG. 5. Panels (a)–(d) show BAM images of the MyA monolayer at 25 °C, 27 °C, 29 °C, and 31 °C, respectively. Panels (e) and (f) show images of the monolayer at two different locations on water at 33 °C. Panels (g) and (h) show images of the monolayer at two different locations on water at 36 °C.

at 25 °C following which the temperature of the monolayer was increased every 5 min. The surface pressure π was simultaneously increased to remain in the coexistence π regime of the L_d to L_o phase transition. This is necessary because the ordered *cis* configuration associated with the L_o phase occurs at progressively higher surface pressures at higher temperatures. Thus, the pressure had to be increased each time the temperature was raised in steps of 1 °C.

Domain morphology and power spectral density function. The BAM data in Fig. 5 shows domain morphology for a single monolayer as a function of temperature. The trend in domain morphology is also reflected in the power spectra of Fig. 7, where Fig. 7(a) shows the power spectra between 26 °C and 36 °C, Fig. 7(b) shows the peak positions, and Figs. 7(c) and 7(d) show the power spectra for $T \approx T_c$ on a log-log scale.

Based on BAM and power spectral density analysis, similar to our earlier case for several MyA monolayers, we could extract three temperature regimes for the present case. These temperature regimes lie in the region $T < T_c$ and $T \approx T_c$.

The region $T < T_c$ can be further subdivided into two T regimes: T far below T_c($T < 27\,^{\circ}$C) and T approaching T_c ($27\,^{\circ}\text{C} \leqslant T \leqslant 32\,^{\circ}$C).

(a) $T < 27\,^{\circ}C$. The monolayer exhibited nearly homogeneous, large sized circular L_o domains in the L_d to L_o coexistence region [Fig. 5(a)], and the corresponding spectrum shows a sharp, single peak in this T regime [Fig. 7(a)].

(b) $27\,^{\circ}C \leqslant T \leqslant 32\,^{\circ}C$. The pressure jump resulted in formation of fingering and dendritic L_o phase domains [Figs. 5(b)–5(d)]. These domains, however, when maintained at constant π, turned circular within few minutes [Figs. 6(a)–6(c)]. Simultaneously, with time (at constant π) a decrease in domain size was observed that could be associated with a continuous loss of MyA molecules from the L_o phase into the L_d phase. The corresponding power spectra show broad, multiple peaked spectra with onset of fractal structures at 27 °C followed by a sharp peak shift to large q values corresponding to the occurrence of a large number of small sized domains in the fluctuation regime at 32 °C [Figs. 7(a) and 7(b)].

$T \approx T_c$

(c) $33\,^{\circ}C \leqslant T \leqslant 36\,^{\circ}C$. Above 32 °C domains of various sizes coexisted in the monolayer [Figs. 5(e)–5(h)]. Reverting to circular structures that occurred rapidly at lower temperatures slowed down when temperatures reached close to 34 °C, where at last fractal morphologies became stable [Figs. 6(d)–6(f)]. A competition thus exists between circular and noncircular fractal structures, the former favored at lower temperatures because of an overall decrease in the total line tension associated with domain boundaries, while the latter favored for an increase in the overall entropy of the monolayer at high T. The power spectra shifts towards low q values, as seen in Figs. 7(a) and 7(b). W_r scales as a power law as $W_r(q) \approx q^{2x}$, with $x \approx 1$ in this regime. We should mention here that since no further purification of the fatty acid was carried out, it may contain very small amounts of impurities that are hard to detect, especially if they are fatty acids of different tail lengths, which is a very likely source. Such small impurities will tend to collect at the domain boundaries and may serve to enhance both the circular and the dendritic structures.

As far as the ergodic nature of the system is concerned, a correspondence existed between the monolayer response in both cases discussed above, i.e., when studies were conducted on identical copies of the monolayer at several temperatures

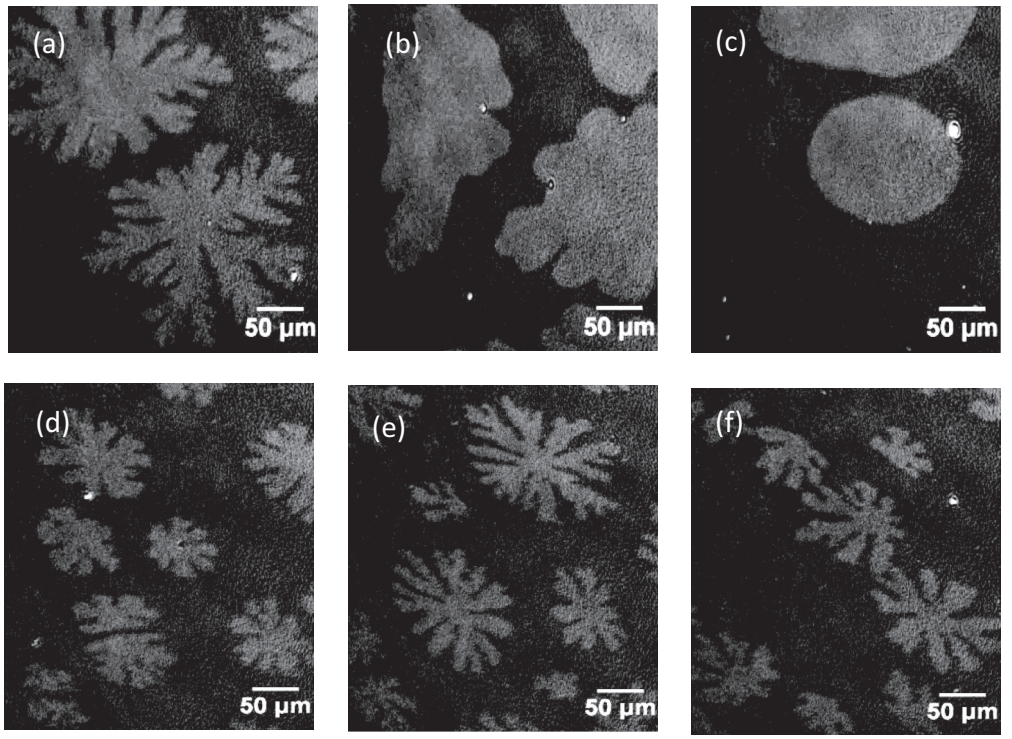

FIG. 6. Panels (a)–(c) show BAM images of the MyA monolayer at 27 °C and (d)–(f) show images of the monolayer at 34 °C within (a) 0 min, (b) 2 min, and (c) 4 min of time evolution at constant π.

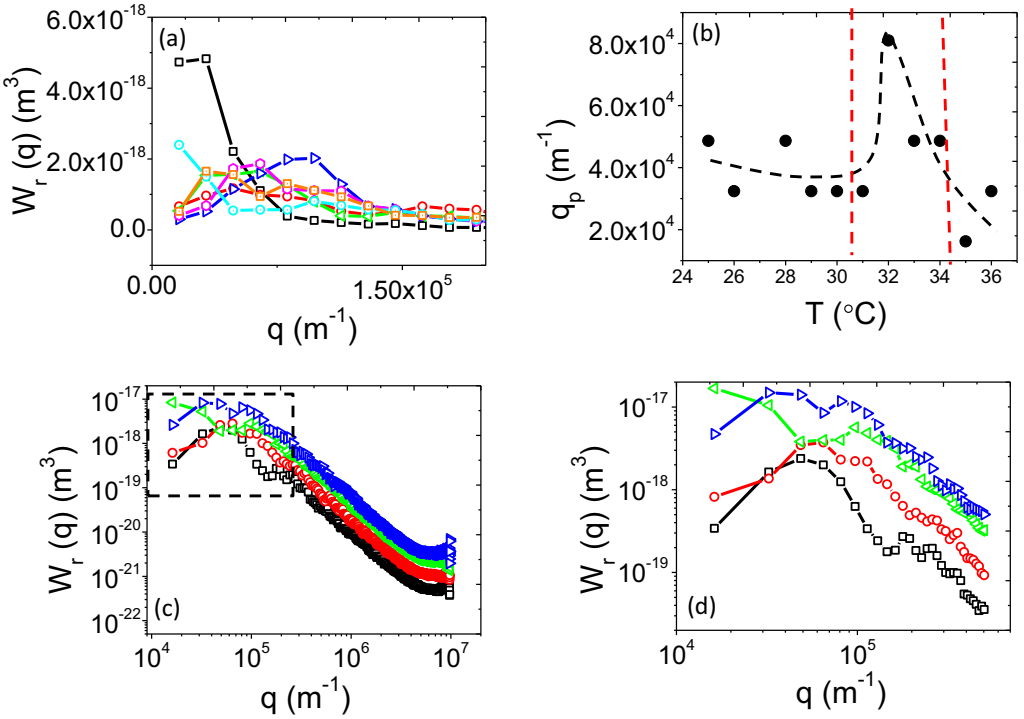

FIG. 7. Power spectral density function (W_r) plotted as a function of q at (a) 26 °C (black squares), 28 °C (red circles), 30 °C (green left triangles), 32 °C (blue right triangles), 34 °C (magenta diamonds), 35 °C (cyan dotted circles), and 36 °C (orange dotted squares). (b) Plot of the peak q position as a function of T (for multiple peaked spectra, peak position at lowest q value is plotted), where the fluctuation regime is enclosed within vertical lines. (c) W_r plotted as a function of q on a log-log scale for $T \approx T_c$ at 33 °C (black squares), 34 °C (red circles), 35 °C (green left triangles), and 36 °C (blue right triangles). Sections of spectra (c), at low q values (in the dashed box) are shown in (d). The spectra in (c) and (d) are upshifted by arbitrary amounts for visualization.

and when a single monolayer was subjected over time to a continuous temperature rise. As the critical point was approached a large number of small sized domains were formed in both cases and it became increasingly difficult to achieve the L_o phase via compression. Finally, close to T_c, the dendritic structure appeared and became stable. Above the critical temperature phase boundaries disappeared and only a single phase occurred for all surface pressures below the collapse pressure of the monolayer. However, in a single monolayer, this happened at $T > 36\,^{\circ}$C, two degrees lower than that obtained in our earlier case for several monolayers. This difference from the previously obtained value of T_c is a departure from strict ergodicity and points to the nonequilibrium nature of the 2D L_d to L_o transition.

IV. CONCLUSION

Here we have approached critical behavior in pristine MyA monolayers from both macroscopic and mesoscopic viewpoints. Within the macroscopic approach we have studied isotherms of the monolayer as a function of temperature in order to locate the critical point and studied the corresponding behavior of the order parameter associated with the L_d to L_o phase transition as this estimated critical point is approached. For the mesoscopic viewpoint we have studied the Brewster angle microscopy images and studied changes in domain morphology to locate the critical regime. The BAM images were quantitatively analyzed by plotting the corresponding power spectra. Three distinct regimes—far from critical, precritical fluctuating, and critical—were identified from both isotherms as well as microscopy data. The critical temperature was thus obtained independently from both macroscopic and mesoscopic measurements of an ensemble of MyA monolayers (ensemble approach). Both these approaches yielded the same value for T_c (at $38\,^{\circ}$C) and thus were found to be consistent lending weight to the conclusion that the value of T_c for the L_d to L_o phase transition in the MyA monolayer is, in fact, higher than that obtained earlier by Suresh *et al.* The system was found to be not strictly ergodic as the critical point estimated by studying several copies of the monolayer was approximately 2° above that obtained by studying the temperature response of a single MyA monolayer. This is due to the nonequilibrium nature of the phase transition. Further, from the comparison of our studies with those on lipid monolayers, we find that the critical regime in their studies is morphologically similar to the precritical regime in our studies. However, this precritical regime precedes true criticality that is associated with stable dendritic structures, which is finally followed (on further increase in temperature) by the disappearance of phase boundaries. The pronounced dendritic morphology in the case of MyA can be a possible result of large surface correlations. The 2D Ising model to which the MyA monolayer was found to conform indicates that the dipolar lattice gas model, which has been used successfully to explain phase transitions in Langmuir monolayers [25–27], can be used for the explanation of critical behavior in this particular system as well. Further, it may be noted that the 2D Ising model is topologically invariant with the Bethe lattice, a lattice structure to model dendritic morphology, which can be a possible explanation for dendritic domain morphology being widespread in such systems.

ACKNOWLEDGMENTS

M. Choudhuri thanks Rajendra Prasad Giri (S.I.N.P.) for assistance, the director of S.I.N.P., and C.S.I.R. (India) for research support.

[1] H. Nishimori and G. Ortiz, *Elements of Phase Transitions and Critical Phenomena* (Oxford University Press, Oxford, UK, 2010).

[2] C. Domb and M. S. Green, *Phase Transitions and Critical Phenomena* (Academic Press, London, 1972), Vol. 2.

[3] D. I. Uzunov, *Introduction to the Theory of Critical Phenomena: Mean Field, Fluctuations and Renormalization* (World Scientific, Singapore, 2010).

[4] L. P. Kadanoff, W. Götze, D. Hamblen, R. Hecht, E. A. S. Lewis, V. V. Palciauskas, M. Rayl, J. Swift, D. Aspnes, and J. W. Kane, Static phenomena near critical points: Theory and experiment, Rev. Mod. Phys. **39**, 395 (1967).

[5] M. C. Cross and P. C. Hoheberg, Pattern formation outside of equilibrium, Rev. Mod. Phys. **65**, 851 (1993).

[6] A. R. Honerkamp-Smith, B. B. Machta, and S. L. Keller, Experimental Observations of Dynamic Critical Phenomena in a Lipid Membrane, Phys. Rev. Lett. **108**, 265702 (2012).

[7] S. L. Veatch, P. Cicuta, P. Sengupta, A. Honerkamp-Smith, D. Holowka, and B. Baird, Critical fluctuations in plasma membrane vesicles, ACS Chem. Biol. **3**, 287 (2008).

[8] S. L. Veatch, O. Soubias, S. L. Keller, and K. Gawrisch, Critical fluctuations in domain-forming lipid mixtures, Proc. Natl. Acad. Sci. USA **104**, 17650 (2007).

[9] A. R. Honerkamp-Smith, S. L. Veatch, and S. L. Keller, An introduction to critical points for biophysicists; observations of compositional heterogeneity in lipid membranes, Biochim. Biophys. Acta **1788**, 53 (2009).

[10] A. R. Honerkamp-Smith, P. Cicuta, M. D. Collins, S. L. Veatch, M. den Nijs, M. Schick, and S. L. Keller, Line tensions, correlation lengths, and critical exponents in lipid membranes near critical points, Biophys. J. **95**, 236 (2008).

[11] V. M. Kaganer, H. Möhwald, and P. Dutta, Structure and phase transitions in Langmuir monolayers, Rev. Mod. Phys. **71**, 779 (1999).

[12] C. M. Knobler and R. C. Desai, Phase transitions in monolayers, Annu. Rev. Phys. Chem. **43**, 207 (1992).

[13] S. Rivière, S. Hénon, J. Meunier, D. K. Schwartz, M.-W. Tsao, and C. M. Knober, Textures and phase transitions in Langmuir monolayers of fatty acids. A comparative Brewster angle microscope and polarized fluorescence microscope study, J. Chem. Phys. **101**, 10045 (1994).

[14] L. K. Nielsen, T. Bjørnholm, and O. G. Mouritsen, Thermodynamic and real-space structural evidence of a 2D critical point in phospholipid monolayers, Langmuir **23**, 11684 (2007).

[15] L. K. Nielsen, T. Bjørnholm, and O. G. Mouritsen, Fluctuations caught in the act, Nat. Commun. **404**, 352 (2000).

[16] N. K. Adam and G. Jessop, The structure of thin films. Part VIII. Expanded films, Proc. R. Soc. London, Ser. A **112**, 362 (1926).

[17] K. A. Suresh, J. Nittmann, and F. Rondelez, Pattern formation during phase transition in Langmuir monolayers near critical temperature, Europhys. Lett. **6**, 437 (1988).

[18] S. Akamatsu and F. Rondelez, Two-dimensional pattern formation in Langmuir monolayers, Prog. Colloid Polym. Sci. **89**, 209 (1992).

[19] D. Hönig and D. Möbius, Reflectometry at the Brewster angle and Brewster angle microscopy at the air-water interface, Thin Solid Films **210-211**, 64 (1992).

[20] S. Hénon and J. Meunier, Microscope at the Brewster angle: direct observation of first-order phase transitions in monolayers, Rev. Sci. Instrum. **62**, 936 (1991).

[21] D. Andelman, F. Broçard, and J. F. Joanny, Phase transitions in Langmuir monolayers of polar molecules, J. Chem. Phys. **86**, 3673 (1987).

[22] H. Möhwald, *Phospholipid Monolayers In Handbook of Biological Physics: Structure and Dynamics of Membranes* (Elsevier Science, Amsterdam, 1995), Vol. 1A.

[23] G. A. Hawkins and G. B. Benedek, Measurement of the Equation of State of a Two-Dimensional Gas Near its Critical Point, Phys. Rev. Lett. **32**, 524 (1974).

[24] N. R. Pallas and B. A. Pethica, Liquid-expanded to liquid-condensed transitions in lipid monolayers at the air/water interface, Langmuir **1**, 509 (1985).

[25] M. M. Hurley and S. J. Singer, Domain-array melting in the dipolar lattice gas, Phys. Rev. B **46**, 5783 (1992).

[26] A. D. Stoycheva and S. J. Singer, Scaling theory for two-dimensional systems with competing interactions, Phys. Rev. E **64**, 016118 (2001).

[27] F. W. J. Weig, P. V. Coveney, and B. M. Boghosian, Lattice-gas simulations of minority-phase domain growth in binary immiscible and ternary amphiphilic fluids, Phys. Rev. E **56**, 6877 (1997).